Journal of Engineering Mechanics. Submitted June 9, 2010; accepted October 17, 2011;
posted ahead of print October 20, 2011. doi:10.1061/(ASCE)EM.1943-7889.0000347

Title: Out-of-plane behavior of one-way spanning unreinforced masonry walls

Hossein Derakhshan[1], Michael C. Griffith[2], and Jason M. Ingham[3], M.ASCE

ABSTRACT

An analytical model is developed to describe the out-of-plane response of one-way spanning unreinforced masonry (URM) walls by investigating the effects of various parameters. Horizontal crack height, masonry compressive strength, and diaphragm support stiffness properties are assumed as variables, and sensitivity analyses are performed to study the influence of these parameters on the cracked wall characteristic behavior. The parametric studies show that crack height significantly influences wall stability by affecting both the instability displacement and the wall lateral resistance. The reduction in cracked wall lateral resistance and in the instability displacement due to finite masonry compressive strength is shown to be significantly amplified by the applied overburden. A study using the typical configuration of flexible diaphragms and URM walls indicates that the wall top support flexibility does not significantly influence cracked wall out-of-plane response. An existing simplified wall behavioral model is improved, and a procedure is proposed for calculation of the wall out-of-plane response envelope.

[1] Ph.D. student, Department of Civil & Environmental Engineering, University of Auckland, Private Bag 92019, Auckland 1010, New Zealand, hder004@aucklanduni.ac.nz

[2] Professor, School of Civil, Environmental, and Mining Engineering, University of Adelaide, SA 5005, Australia, mcgrif@civeng.adelaide.edu.au

[3] Associate Professor, Department of Civil & Environmental Engineering, University of Auckland, Private Bag 92019, Auckland 1010, New Zealand, j.ingham@auckland.ac.nz

Journal of Engineering Mechanics. Submitted June 9, 2010; accepted October 17, 2011;
posted ahead of print October 20, 2011. doi:10.1061/(ASCE)EM.1943-7889.0000347

CE Database subject headings: Brick masonry; Walls; Flexural strength; Lateral loads; Axial loads; Stiffness; Seismic analysis

INTRODUCTION

In the simplified seismic assessment of URM walls loaded in their out-of-plane direction, the wall is represented as a one-way vertically spanning element, with wall damage being in the form of a horizontal crack occurring at an intermediate height. This cracking pattern is not considered a failure, and instead a stable out-of-plane rocking wall mechanism is anticipated to form following the initial damage.

Detailed characterization of wall post-cracking response is important as part of seismic evaluation procedures that are based on restricting the wall rocking displacement to the cracked wall displacement capacity. Doherty (2000) analyzed the dynamic behavior of a cracked URM wall using a single-degree-of-freedom (SDOF) system, which had trilinear stiffness properties. Griffith et al. (2003) developed a method for seismic analysis of similar walls using a substitute linear elastic structure, and the method requires the wall trilinear behavior as input information. Lawrence et al. (2009) and Derakhshan et al. (2009) used similar models for earthquake design of URM buildings and for seismic evaluation of URM walls, respectively.

Simplified bilinear (Blaikie 1999; Simsir 2004; Priestley et al. 2007) or trilinear (Doherty 2000) models have not addressed or quantified various aspects of wall rocking response. These areas of required research include investigating the effects of applied overburden, wall thickness, finite masonry compressive strength, horizontal crack height, and wall support flexibility. The most

Journal of Engineering Mechanics. Submitted June 9, 2010; accepted October 17, 2011;
posted ahead of print October 20, 2011. doi:10.1061/(ASCE)EM.1943-7889.0000347

comprehensive available predictive model is that proposed by Doherty (2000), but that model does not address most of the aforementioned parameters and a more comprehensive formulation enables use of the developed models for a wider variety of URM walls. The aim of this study was to formulate a general analytical approach to describe wall characteristic behavior, with a companion experimental campaign undertaken to support the presented findings. The aforementioned bilinear and trilinear models are extended to incorporate variable crack height, masonry compressive strength, and a flexible top support.

Experimental shake table testing of single-storey URM walls connected to a flexible diaphragm (Simsir 2004) or to a rigid top support (Meisl et al. 2007) showed that one-way bending URM walls crack at above mid-height (approximately at two-thirds wall height from base), when subjected to out-of-plane inertial forces. Various parameters including differential support accelerations above and below the wall and decreasing overburden up the wall height contribute to the crack height.

As the upper and lower wall segments displace out-of-plane, a pivot is formed at the intermediate height crack, resulting in a much higher compressive stress being developed than that occurring in the undeformed wall. As a result of finite masonry compressive strength, a stress block is formed at the pivot and the line of action of the resultant axial compression force is displaced toward the wall centerline. This variation in compression eccentricity unfortunately results in a reduction in the moment arm of the wall self-weight and applied overburden, which in turn reduces the wall restoring moments.

Journal of Engineering Mechanics. Submitted June 9, 2010; accepted October 17, 2011;
posted ahead of print October 20, 2011. doi:10.1061/(ASCE)EM.1943-7889.0000347

Past earthquakes have shown that the diaphragm in-plane stiffness significantly affects the seismic response of existing masonry buildings (Brignola et al. 2009). Although investigating the dynamic effects of flexible diaphragms was outside the scope of this study, a flexible support is included in the formulation of the static response, and the significance of diaphragm flexibility in altering wall push-over response by modifying the wall displaced geometry is investigated.

UNCRACKED BEHAVIOR

Although current seismic assessment guidelines (ASCE 2007; NZSEE 2006) recommend wall evaluation for out-of-plane behavior based on a cracked section analysis, investigation of wall uncracked behavior may result in a more economical wall assessment for areas of low seismicity, and the study is necessary when estimating seismic force demand for wall-diaphragm connections.

Fig. 1 shows an URM wall subject to out-of-plane uniform forces, which is a simple and realistic representation of seismic inertial forces (Priestley 1985). Experimental shake table test results (Doherty 2000) suggested that the assumption of uniformly distributed lateral face loads led to overestimation of wall behavior by approximately 20% and 10%, respectively, when the wall was subjected to overburden stresses of 75 kPa and 150 kPa. It is considered appropriate for the purpose of this parametric study to assume uniformly distributed forces, and a procedure to compensate for this approximation when deriving the governing equation of dynamic motion is given in Doherty (2000, pp. 175-179).

Journal of Engineering Mechanics. Submitted June 9, 2010; accepted October 17, 2011;
posted ahead of print October 20, 2011. doi:10.1061/(ASCE)EM.1943-7889.0000347

The wall has unit length and a mass of m_o per unit height, and is subject to overburden, O. Maximum tensile strength in the wall cross section can be obtained using basic mechanics, assuming elastic behavior and homogenized section properties,

$$\sigma^T(x) = \frac{M(x)t}{2I_g} - \frac{P(x)}{t} \tag{1}$$

where t is the effective wall thickness and is equal to $t = t_n - 2p$, with t_n being the nominal wall thickness and p being the depth of mortar pointing at each wall face. $M(x)$ and $P(x)$ are, respectively, the height-dependent bending moment and axial load, and I_g is the cross section moment of inertia equal to $t^3/12$. Substituting these force resultants based on statics,

$$\sigma^T(x) = 3\frac{whx - wx^2}{t^2} - \frac{(h-x)m_0 g + O}{t} \tag{2}$$

where h is the total wall height.

The location of the wall maximum tensile stress is obtained by finding the wall height, x, at which the extremum of σ^T occurs. This wall height is the theoretical location of wall cracking and is obtained as,

$$x_{cr} = \frac{h}{2} + \frac{m_0 g t}{6w_{cr}} \tag{3}$$

where w_{cr} is the uniformly applied wall cracking force, and the magnitude of this force is found by assuming the maximum tensile stress to be equal to the masonry bond strength, i.e. $\sigma^T(x) = f'_{fb}$ in Eq. 2. Therefore,

$$f'_{fb} = \frac{3}{4}w_{cr}\left(\frac{h}{t}\right)^2 + \frac{(m_0 g)^2}{12w_{cr}} - \frac{m_0 g h}{2t} - \frac{O}{t} \tag{4}$$

Journal of Engineering Mechanics. Submitted June 9, 2010; accepted October 17, 2011;
posted ahead of print October 20, 2011. doi:10.1061/(ASCE)EM.1943-7889.0000347

Two solutions for the cracking force w_{cr} are obtained when solving Eq. 4. One of these solutions is close to zero, and the acceptable solution is approximately 10^4 times the first algebraic solution. The acceptable solution for w_{cr} is:

$$w_{cr} = \frac{f_{fb}^{'} + \frac{O}{t} + 0.5\frac{m_0 gh}{t} + \sqrt{(f_{fb}^{'} + \frac{O}{t})(f_{fb}^{'} + \frac{O}{t} + \frac{m_0 gh}{t})}}{1.5(\frac{h}{t})^2} \quad (5)$$

Fig. 2 shows the variation of crack height ratio, $\beta = x_{cr}/h$, for a typical two-leaf URM wall (t = 210 mm, h = 4100 mm, $f_j^{'}$ = 2 MPa, and ρ_m = 1800 kg/m^3), assuming three different ratios of the applied overburden load to wall weight, $\psi = O/W$. Fig. 2 shows that β is particularly sensitive to low values of $f_{fb}^{'}$, especially for the case when zero overburden is applied. Shaking table testing programs conducted by both Simsir (2004) and Meisl et al. (2007) have experimentally established values for β that were approximately 20% higher than those predicted by Fig. 2 (respectively, 0.7 and 0.63 instead of 0.58 and 0.52 calculated using Fig. 2). A series of static airbag tests reported by Derakhshan (2011) resulted in an average crack height ratio of 0.58, being 7% higher the average value of 0.54 calculated using Fig. 2. Previously obtained experimental data suggests that the location of header courses does not directly affect the crack height ratio. While static airbag tests conducted by Derakhshan (2011) resulted in cracks occurring in a stretcher course in all tested two-leaf walls (5 walls in total) and three-leaf walls (3 walls in total), Meisl et al. (2007) reported that all 4 walls tested on a shake table cracked at a header course.

Journal of Engineering Mechanics. Submitted June 9, 2010; accepted October 17, 2011;
posted ahead of print October 20, 2011. doi:10.1061/(ASCE)EM.1943-7889.0000347

The wall total cracking force, $F_{cr} = hw_{cr}$, is obtained by solution of the parabolic equation for w_{cr}, and ignoring the displacements that occur due to top support flexibility, the wall maximum displacement at the state of cracking can be obtained as,

$$\Delta_{ucr} = \frac{5F_{cr}h^3}{384EI_g} \tag{6}$$

where E is the homogenized modulus of elasticity of masonry.

POST-CRACKING BEHAVIOR

The out-of-plane resistance of cracked URM walls is predominantly attributed to the restoring effects of wall self-weight and applied overburden. The eccentricity of the applied gravity forces controls the moment arm, thus affecting the wall stability. In a cyclic loading pattern, the overall stabilizing effect of the gravity forces reduces with increasing eccentricity.

Fig. 3 shows a free body diagram of a cracked wall having an effective length of l_e as defined later, and both the overburden and weight forces are assumed to apply at the wall centerline. The horizontal reaction H_C (labeled in Fig. 3) was found by taking moments about point A (distance of $0.5c_1a$ from wall edge):

$$hH_C + O_e(\frac{t}{2} - \Delta_t - \frac{c_1a}{2}) + (1-\beta)W_e(\frac{t-\Delta_m-\Delta_t+c_1a}{2}) + \beta W_e(\frac{t-\Delta_m-c_1a}{2}) - w_e\frac{h^2}{2} = 0 \tag{7}$$

$$H_C = w_e\frac{h}{2} - \frac{O_e}{2h}(t-2\Delta_t-c_1a) + (1-\beta)W_e\frac{\Delta_t}{2h} + W_e(\frac{\Delta_m-t+c_1a}{2h}) \tag{8}$$

H_A is found by equating the horizontal forces:

Journal of Engineering Mechanics. Submitted June 9, 2010; accepted October 17, 2011;
posted ahead of print October 20, 2011. doi:10.1061/(ASCE)EM.1943-7889.0000347

$$H_A = w_e h - H_C = w_e \frac{h}{2} + \frac{O_e}{2h}(t - 2\Delta_t - c_1 a) - (1-\beta) W_e \frac{\Delta_t}{2h} - W_e(\frac{\Delta_m - t + c_1 a}{2h}) \quad (9)$$

Taking moments about point B (distance of $0.5a$ from wall edge) of the top free body (Fig. 4),

$$(1-\beta) h H_C - O_e(\frac{t-a}{2} - \Delta_m + \Delta_t) - (1-\beta) W_e(\frac{t - \Delta_m + \Delta_t - a}{2}) - w_e(1-\beta)^2 \frac{h^2}{2} = 0 \quad (10)$$

Substituting H_C from Eq. 8 and rearranging,

$$w_e = \frac{2}{\beta h^2}\left[W_e(t - \Delta_m + \frac{\beta\Delta_t}{2} - \frac{1+c_1}{2} a) + \frac{O_e}{1-\beta}((1-0.5\beta)t - \Delta_m + \beta\Delta_t - (1 + c_1 - c_1\beta)\frac{a}{2}) \right] \quad (11)$$

where Δ_m and Δ_t are, respectively, maximum wall mid-height displacement and wall top displacement, which are assumed to occur at diaphragm mid-span. As Δ_t is dictated by the reaction of the top support, H_C, the displacement value can be represented in Eq. 11 in the form of force quantities, ultimately resulting in Eq. 13 that includes only one displacement variable (Δ_m). Wall deformation at the top support is governed by:

$$\Delta_t = \frac{H_C}{K_D} \quad (12)$$

where K_D is a linear representation corresponding to the diaphragm stiffness at its mid-span displacement and loaded with a uniformly distributed force. Replacing Δ_t from Eq. 12 into Eq. 11, and defining an auxiliary parameter, η,

$$w_e = \frac{2}{\beta h^2}\left[W_e(t - \Delta_m - \frac{1+c_1}{2} a) + \frac{O_e}{1-\beta}((1-0.5\beta)t - \Delta_m - (1 + c_1 - c_1\beta)\frac{a}{2}) \right]$$

$$+ \frac{2}{\beta h^2}[\eta(w_e h^2 + W_e(\Delta_m - t + c_1 a) - O_e(t - c_1 a))] \quad (13)$$

where η is:

Journal of Engineering Mechanics. Submitted June 9, 2010; accepted October 17, 2011;
posted ahead of print October 20, 2011. doi:10.1061/(ASCE)EM.1943-7889.0000347

$$\eta = \frac{\beta}{1-\beta}\frac{O_e + 0.5(1-\beta)W_e}{2hK_D - (1-\beta)W_e - 2O_e} \tag{14}$$

Solving Eq. 13 for w,

$$w_e = \frac{2W_e}{(1-\frac{2\eta}{\beta})\beta h^2}[(t-\Delta_m)(1-\eta) - (1+c_1-2c_1\eta)\frac{a}{2}]$$

$$+\frac{2O_e}{\beta(1-\beta)(1-\frac{2\eta}{\beta})h^2}[t(1-0.5\beta-\eta(1-\beta)) + \eta(1-\beta)c_1 a - \Delta_m - (1+c_1-c_1\beta)\frac{a}{2}] \tag{15}$$

Rearranging Eq. 15, the intermediate crack height displacement, Δ_m, is obtained as:

$$\Delta_m = \frac{\beta(\frac{2\eta}{\beta}-1)h^2 w_e}{2W_e(1-\eta+\frac{\psi}{1-\beta})} + t\frac{1-\eta-\frac{(1+c_1-2c_1\eta)a}{2t}+\psi[\frac{1-0.5\beta}{1-\beta}-\eta+(\eta c_1-\frac{1+c_1-c_1\beta}{2(1-\beta)})\frac{a}{t}]}{1-\eta+\frac{\psi}{1-\beta}} \tag{16}$$

Wall effective length

Consistent values of wall and diaphragm stiffness should be used when evaluating wall behavior. With some approximations, the wall stiffness can be defined as the combined effect of an infinite number of infinitesimal wall strips spanning vertically between the diaphragm and the ground. The generalized coordinate principles (Clough and Penzien, 2003) can be used to define effective lateral wall stiffness, and the constraint between the wall and diaphragm suggests that wall deformation follows that of the timber diaphragm. Assuming linear behavior, the effective wall length for the purpose of generalized wall stiffness calculations is obtained as:

$$l_e = 2\int_0^{0.5L} \phi(x)^2 dx \tag{17}$$

Journal of Engineering Mechanics. Submitted June 9, 2010; accepted October 17, 2011;
posted ahead of print October 20, 2011. doi:10.1061/(ASCE)EM.1943-7889.0000347

where L is the diaphragm span, and $\phi(x)$ is the shape function dictated by the shear deformation of the timber diaphragm when subjected to uniform lateral forces:

$$\phi(x) = \frac{8}{L^2}\left(\frac{Lx}{2} - \frac{x^2}{2}\right) \tag{18}$$

and therefore

$$l_e = \frac{8}{15}L \tag{19}$$

A method for linear representation of wall nonlinear behavior has been suggested by Griffith et al. (2003).

A generalized stiffness is obtained for the timber diaphragm stiffness (see also Ingham et al., 2011) as:

$$K_D = \frac{16}{3}\frac{G_e A}{L\kappa} \tag{20}$$

where G_e and A are, respectively, diaphragm equivalent shear modulus and cross section area, and κ is the shear coefficient. Timber diaphragm deformation is a result of timber board flexure and nail deformation and slip (NZSEE, 2006). Brignola et al. (2009) conducted a parametric study that suggested an equivalent shear modulus of 2.5 MPa to 30 MPa for several combinations of timber board thickness, joist spacing, and nail diameters, spacing, and deformability. The equivalent shear modulus can be used in shear stiffness equations in the form of Eq. 20 to account for overall in-plane stiffness of timber diaphragm. Assuming the suggested range of equivalent shear modulus, timber board thickness of 20 mm to 30 mm, and diaphragm aspect ratio (width, B, to span, L) of between 0.5 and 1, a range of diaphragm stiffness values between 2/3 kN/mm and 32/3 kN/mm can be obtained.

Journal of Engineering Mechanics. Submitted June 9, 2010; accepted October 17, 2011;
posted ahead of print October 20, 2011. doi:10.1061/(ASCE)EM.1943-7889.0000347

Discussion on wall behavior

Observations made on the results generated by Eq. 12, Eq. 15, and Eq. 16 showed that for typical URM wall dimensions and timber diaphragm stiffness properties (t = 210 mm, h = 4100 mm, L = 8000 mm, $f_j^{'}$=2 MPa, $K_D = 2/3$ kN/mm or $K_D = 32/3$ kN/mm, $\psi = 0$, $a/t = 0.1$, $\beta = 2/3$, and $\rho_m = 1800$ kg/m^3), Δ_t remained relatively close to zero while Δ_m increased until an instability mechanism was formed in the wall. Due to the top wall displacement, Δ_t, being negligible comparing to Δ_m, the wall out-of-plane behavior is closely represented by the case where the top support is rigid. This analysis assumes that the effect of inertial forces applied on the diaphragm mass is insignificant. While this assumption is realistic for URM buildings with light weight timber diaphragms, further studies are recommended to include buildings with significant diaphragm mass.

Simplifications for rigid top support

For a fully rigid wall top support ($K_D \to \infty$), η is obtained as zero from Eq. 14. Substituting $\eta = 0$ in Eq. 15, renaming Δ_m with a more general Δ, and assuming unit wall length:

$$w = \frac{W}{(\beta - \beta^2)h^2}[2(1-\beta)(t - \Delta - \frac{1+c_1}{2}a) + \psi((2-\beta)t - 2\Delta + (c_1\beta - c_1 - 1)a)] \qquad (21)$$

Eq. 21 results in the maximum lateral force resistance (Eq. 22), and instability displacement (Eq. 23), respectively if zero displacement and zero lateral force are assumed:

$$w_{\max} = \frac{Wt}{(\beta - \beta^2)h^2}[2(1-\beta)(1 - \frac{1+c_1}{2}\frac{a}{t}) + \psi(2 - \beta + (c_1\beta - c_1 - 1)\frac{a}{t})] \qquad (22)$$

Journal of Engineering Mechanics. Submitted June 9, 2010; accepted October 17, 2011;
posted ahead of print October 20, 2011. doi:10.1061/(ASCE)EM.1943-7889.0000347

$$\Delta_{ins} = t\frac{1-\frac{(1+c_1)a}{2t}+\psi\left(\frac{1-0.5\beta}{1-\beta}-\frac{1+c_1-c_1\beta}{2(1-\beta)}\frac{a}{t}\right)}{1+\frac{\psi}{1-\beta}} \tag{23}$$

As some of the parameters in Eq. 22 and Eq. 23 are interdependent, the analysis is developed further by obtaining a/t and c_1 as functions of β and ψ. Parameter a is calculated using the stress block diagram shown in Fig. 4:

$$a = \frac{W}{0.85 f_j^{'}}(1-\beta+\psi) \tag{24}$$

Substituting $\rho_m = 1800$ kg/m^3, a is obtained in mm units as:

$$a = \frac{18\times10^{-06} h t_n}{0.85 f_j^{'}}(1-\beta+\psi) \tag{25}$$

where $f_j^{'}$ is the mortar compressive strength (MPa), h is the wall height (mm), and t_n is the wall nominal thickness (mm).

Coefficient c_1 is obtained from Fig. 4 as:

$$c_1 = \frac{O+W}{O+(1-\beta)W} = \frac{1+\psi}{1-\beta+\psi} \tag{26}$$

By obtaining a and c_1 from Eq. 25 and Eq. 26, $w_{\max}$ and Δ_{ins} can be calculated using Eq. 22 and Eq. 23 respectively.

Influence of β on wall characteristic behavior

The sensitivity of Eq. 22 and Eq. 23 to crack height ratio was investigated, and was shown to be significant for a typical two-leaf URM wall ($t = 210$ mm, $h = 4100$ mm, $f_j^{'} = 2$ MPa,

Journal of Engineering Mechanics. Submitted June 9, 2010; accepted October 17, 2011;
posted ahead of print October 20, 2011. doi:10.1061/(ASCE)EM.1943-7889.0000347

$W = 20$ kN). Fig. 5 and Fig. 6 show the variation of wall lateral resistance and instability displacement over a reasonable range of crack heights. Fig. 5 shows that the wall resistance has a parabolic relationship with β, and that increasing β within a reasonable range generally decreases the maximum wall resistance. Similarly, Fig. 6 shows that varying β has a considerable effect on the instability displacement, particularly for higher values of overburden ratio. The sharp decrease in the wall instability displacement due to elevated overburden and high crack height is explained using Fig. 4. Increased overburden results in an increased value of a, which reduces the moment arm of the restoring forces (d_5) and increases the moment arm of the overturning forces (d_4). In parallel, as β increases, both d_5 and the restoring forces $(1-\beta)W$ decrease due to the geometry of the wall top segment. The combined effect of these factors results in the wall instability displacement decreasing sharply. A decrease in d_4 does not affect the existing overturning moments when no overburden is applied, and thus reduction in the wall instability displacement is not as significant for walls having no overburden loads applied when compared with walls having overburden loads applied.

An example scenario is considered with the previously specified two-leaf wall having an overburden load applied ($\psi = 0.75$). An increase in β from 0.5 to 0.7 results in a decrease in the wall maximum resistance and instability displacement, respectively by 13% and 11%. A reduction in the instability displacement decreases the wall displacement capacity, and a reduction in the wall lateral resistance increases displacement demand on the wall, with these combined relationships resulting in a sharp decrease in wall post-cracking stability. Considering the shake table testing results obtained by Simsir (2004) and Meisl et al. (2007), it is

Journal of Engineering Mechanics. Submitted June 9, 2010; accepted October 17, 2011;
posted ahead of print October 20, 2011. doi:10.1061/(ASCE)EM.1943-7889.0000347

recommended that a crack height ratio of 0.67 be assumed instead of 0.5 as conventionally used when predicting wall out-of-plane response.

Influence of a/t on wall characteristic behavior

In addition to the study of the effects of β on Eq. 22 and Eq. 23, the influence of finite masonry compressive strength on these equations was also investigated. To facilitate comparison the equations were re-written by assuming $a/t = 0$, and the maximum lateral load, $\hat{w}_{\max}$, and the instability displacement, $\hat{\Delta}_{ins}$, were derived for the case of infinite masonry strength. Therefore,

$$\hat{w}_{\max} = \frac{Wt}{(\beta - \beta^2)h^2}[2(1-\beta) + \psi(2-\beta)] \tag{27}$$

$$\hat{\Delta}_{ins} = t\frac{1 + \psi(\frac{1-0.5\beta}{1-\beta})}{1 + \frac{\psi}{1-\beta}} \tag{28}$$

Dividing Eq. 22 by Eq. 27, a ratio was obtained and defined as *percentage of maximum rigid resistance* (*PMR*):

$$PMR(\%) = \frac{w_{\max}}{\hat{w}_{\max}} \times 100 = 100 \times [1 - \frac{a}{t}(\frac{(1-\beta)(1+c_1) + (1+c_1-c_1\beta)\psi}{2(1-\beta) + (2-\beta)\psi})] \tag{29}$$

Replacing a and c_1, respectively from Eq. 25 and Eq. 26, into Eq. 29, and after simplification,

$$PMR(\%) = 100 - \frac{0.002h}{f_j^{'}}(\psi + \frac{(1-\beta)(2\psi + 2 - \beta)}{2(1-\beta) + (2-\beta)\psi})\frac{t_n}{t} \tag{30}$$

where h and $f_j^{'}$ are in mm and MPa units, respectively. Fig. 7 shows the variation of *PMR* vs. calculated for different ratios of $h/f_j^{'}$. For simplicity, $t = t_n - 20$ mm was assumed to account for mortar pointing, and β was assumed to be equal to $2/3$ (based on studies by Simsir (2004) and

Journal of Engineering Mechanics. Submitted June 9, 2010; accepted October 17, 2011;
posted ahead of print October 20, 2011. doi:10.1061/(ASCE)EM.1943-7889.0000347

Meisl et al. (2007)), although changing β has little effect on the results produced by Eq. 30. The decrease in wall strength for zero overburden was on average 5% for the three assumed $h/f_j^{'}$ ratios, but this decrease wass 25% for an overburden ratio equal to 2. It was concluded that finite mortar compressive strength decreases the cracked wall out-of-plane resistance, and that the decrease in wall resistance is exacerbated by an increase in $h/f_j^{'}$ ratio.

Fig. 8 compares the results produced by Eq. 28 with those obtained from Eq. 23, and the comparison shows that Eq. 28 overestimates wall instability displacement, especially for high levels of overburden. For instance, Δ_{ins}/t for $h/f_j^{'} = 4500$ and $\psi = 1$ is approximated from Fig. 8 to be 0.64, but assuming $h/f_j^{'} = 0$ overestimates the instability displacement ratio by more than 15% ($\Delta_{ins}/t \cong 0.75$).

Eq. 30 includes reduction of the wall lateral resistance due to mortar pointing and infinite masonry compressive strength, but the equation excludes rounding and pre-crushing of brick corners and wall elastic deformations. The effects of such factors can be assessed by experimentation, and a calibration factor of 0.83 was obtained (Derakhshan 2011) for use with Eq. 30 to evaluate the lateral resistance of walls constructed using vintage clay bricks and tested by means of a system of airbags. This calibration factor further decreases the predicted wall lateral resistance, resulting in a 38% reduction for the previous example of an URM wall with overburden ratio equal to 2.

PREDICTIVE MODEL FOR WALL CHARACTERISTIC BEHAVIOR

Journal of Engineering Mechanics. Submitted June 9, 2010; accepted October 17, 2011;
posted ahead of print October 20, 2011. doi:10.1061/(ASCE)EM.1943-7889.0000347

A trilinear elastic model proposed by Doherty (2000) is characterised here to predict the behavior of cracked out-of-plane loaded walls, with the related parameters being shown in Fig. 9. $\hat{F}_0$ and $\hat{\Delta}_{ins}$ are, respectively the total out-of-plane force per wall length ($h\hat{w}_{\max}$) and wall instability displacement assuming infinite masonry strength (Eq. 27 and 28), with the former being simplified for $\beta = 2/3$ and $\rho_m = 1800$ kg/m^3, and unit wall length as,

$$\hat{F}_0 = 53\times10^{-06} t t_n (1+2\psi) \tag{31}$$

where wall thickness and $\hat{F}_0$ are in mm and kN units, respectively. Experimental data are required to calibrate the analytically established formulae, and therefore the results from a series of laboratory static airbag tests conducted on URM walls (Derakhshan 2011) were used for this purpose. The tested walls were constructed using recycled vintage (circa 1880-1930) solid clay bricks, and the walls were initially in an uncracked condition. Several tests were conducted on the uncracked and cracked walls, and the tests produced PMR ratios that were on average 0.83 times that obtained using Eq. 30, due to the roundedness of brick corners and prior masonry crushing at pivotal points. Other factors that contributed to this difference are wall elastic deformations that were neglected in the analytical study. An empirical correction factor of 0.83 is used with Eq. 30, and the equation is re-written for $\beta = 2/3$ as,

$$PMR_{emp}(\%) = 83 - \frac{0.0016h}{f_j^{'}}\left(\frac{\psi^2+\psi+0.33}{\psi+0.5}\right)\frac{t_n}{t} \tag{32}$$

The maximum wall lateral resistance, $F_{\max}$, is equal to the product of PMR_{emp} and $\hat{F}_0$. The idealized maximum force F_i was estimated from the aforementioned test data to be $0.9F_{\max}$.

Journal of Engineering Mechanics. Submitted June 9, 2010; accepted October 17, 2011;
posted ahead of print October 20, 2011. doi:10.1061/(ASCE)EM.1943-7889.0000347

Therefore, multiplying Eq. 31 and Eq. 32, and applying the coefficient 0.9, the trilinear maximum lateral force per unit wall length can be obtained:

$$F_i = 0.9 \times F_{\max} = 39.6 \times 10^{-06} t t_n (1 + 2\psi) - 0.154 t_n^2 \times 10^{-08} \frac{h}{f_j^{'}} (\psi^2 + \psi + 0.33) \tag{33}$$

The wall instability displacement, Δ_{ins}, is obtained from Eq. 23, which is simplified for $\beta = 2/3$ as,

$$\Delta_{ins} = t \frac{1 + 2\psi}{1 + 3\psi} - \frac{7.1 \times 10^{-06} \frac{h}{f_j^{'}} (3\psi^2 + 3\psi + 1)}{1 + 3\psi} t_n \tag{34}$$

Δ_1 is approximated as,

$$\Delta_1 = \frac{5 F_i h^3}{384 E I_{cr}} \tag{35}$$

where I_{cr} is obtained based on experimental data reported by Derakhshan (2011) as,

$$I_{cr} = (0.18\psi + 0.04) I_g \le I_g \tag{36}$$

Δ_1 was calculated for all tests reported by Derakhshan (2011), and the value was observed to be on average 4% of the instability displacement, Δ_{ins}. Therefore, it is recommended to use:

$$\Delta_1 = 0.04 \Delta_{ins} \tag{37}$$

Δ_2 is a point corresponding to F_i on the bilinear rigid rocking curve, as shown in Fig. 9, and the displacement value is obtained as:

$$\Delta_2 = (1 - 0.009 PMR_{emp}) \Delta_{ins} \tag{38}$$

Journal of Engineering Mechanics. Submitted June 9, 2010; accepted October 17, 2011;
posted ahead of print October 20, 2011. doi:10.1061/(ASCE)EM.1943-7889.0000347

A step-by-step procedure is detailed below to obtain an idealized trilinear curve for unit wall length.

Procedure for obtaining trilinear force-displacement curve

Step 1. Establish wall geometry: nominal thickness (including all rendering), effective thickness (equal to the depth of mortar bed-joint), and clear height.

Step 2. Obtain material properties including masonry bond strength, mortar compressive strength, and homogenized modulus of elasticity for masonry. Estimate overburden, O, for unit wall length, and calculate wall weight for unit wall length.

Step 3. Calculate $F_{cr} = hw_{cr}$, with w_{cr} obtained by solution of Eq. 4.

Step 4. Calculate Δ_{ucr} using Eq. 6.

Step 5. Calculate PMR_{emp} using Eq. 32.

Step 6. Calculate F_i using Eq. 33.

Step 7. Calculate instability displacement, Δ_{ins}, using Eq. 34.

Step 8. Calculate Δ_1 and Δ_2, respectively using Eq. 37 and Eq. 38.

Step 9. Plot initial elastic behavior using coordinates (0,0) and (Δ_{ucr}, F_{cr})

Step 10. Plot the trilinear model using coordinates (0,0), (Δ_1, F_i), (Δ_2, F_i), and (Δ_{ins}, 0).

Illustrative examples

Journal of Engineering Mechanics. Submitted June 9, 2010; accepted October 17, 2011;
posted ahead of print October 20, 2011. doi:10.1061/(ASCE)EM.1943-7889.0000347

The developed procedure for calculation of the trilinear idealized response of URM walls was applied to a number of walls, and the results are summarized in Table 1. The constructed models are shown in Fig. 10 and Fig. 11, along with the respective models obtained when the Doherty (2000) method was used. Fig. 12 shows an initial part of Fig. 11 at an expanded scale. A "New" state of degradation of mortar at the cracked bed-joint was assumed when using the method recommended by Doherty (2000), and a comparison between the model obtained for W3 using the method recommended in Doherty (2000) and the model obtained in this study (see Fig. 11) suggests that the former method overestimated the wall instability displacement by 30% (275 mm when compared to 212 mm calculated in this study). The method recommended in Doherty (2000) also resulted in the predicted rocking force for all walls to be approximately 30% greater than that calculated in this study.

As mentioned in the discussion related to Eq. 32, a relatively higher applied overburden and a relatively lower mortar compressive strength both decrease the PMR_{emp} ratio. The combined effect of these two factors resulted in the PMR_{emp} ratio for W3 being 15% lower than the same value for W4 (70% compared to 82%).

A higher value was obtained for the rocking force when compared with the cracking force calculated for W3 (see Fig. 12), but this relationship was reverse for other walls. The cracking force (Eq. 5) is a function of the masonry bond strength, but the rocking force (Eq. 33) is independent of this value. This difference resulted in two different relationships being observed for different example walls, where the rocking force was found to be either higher or lower than the calculated cracking force.

Journal of Engineering Mechanics. Submitted June 9, 2010; accepted October 17, 2011;
posted ahead of print October 20, 2011. doi:10.1061/(ASCE)EM.1943-7889.0000347

Application of the model

The obtained trilinear force-displacement relationship has direct application in simplified dynamic analysis of one-way spanning out-of-plane loaded URM walls connected to rigid supports. The model also has potential (Derakhshan 2011) to be used in a two-degree-of-freedom model, representing the behavior of an URM wall connected to a flexible diaphragm, or in a multi-degree-of-freedom model of a taller URM building.

SUMMARY AND CONCLUSIONS

The out-of-plane behavior of one-way spanning URM walls was investigated for uncracked and cracked conditions. Crack height was found to be particularly sensitive to low values of masonry bond strength, especially for the case when zero overburden is applied. A formulation was obtained which predicted crack height due to static loading with good correlation, but the method underestimated the crack height by on average 20% for walls that were tested on shake tables by previous investigators.

Relationships were obtained to calculate wall force-displacement response, which incorporated the effects of variable crack height, finite masonry compressive strength, and a flexible diaphragm support. A parametric study showed that if diaphragm inertial forces are ignored, a flexible top support does not significantly influence wall out-of-plane resistance, with only minor variation of the wall response when compared to the case of a rigid top support. Sensitivity

Journal of Engineering Mechanics. Submitted June 9, 2010; accepted October 17, 2011;
posted ahead of print October 20, 2011. doi:10.1061/(ASCE)EM.1943-7889.0000347

analyses showed that increasing the crack height above the wall mid-height decreased both the wall instability displacement and the wall lateral out-of-plane resistance.

A formulation was presented which compared the decreased wall maximum resistance due to masonry toe crushing to that assuming infinite masonry strength, and a parametric study showed that this ratio (*PMR*) decreases significantly with increased overburden. The *PMR* ratio was also shown to have a direct relationship with mortar compressive strength, while maintaining an inverse relationship with wall height. A parametric study showed that the wall instability displacement decreases dramatically with increasing overburden ratio.

Prior to calibration based on the experimental data from testing of walls built with vintage bricks, the presented simplified model was used to predict up to 15% and 25% reduction in, respectively, instability displacement and lateral resistance when compared to the case of existing rigid rocking models. The prediction made using the calibrated formula showed a reduction of 38% in the wall lateral resistance for a typical URM wall with an overburden ratio equal to 2.

An existing predictive trilinear model was developed further to describe out-of-plane response for a broader range of URM walls, and a procedure was presented for calculation of the wall out-of-plane response envelope.

Illustrative examples were provided, which compared the predicted wall behavior when the procedure developed in this study was used against the results obtained from a similar model

Journal of Engineering Mechanics. Submitted June 9, 2010; accepted October 17, 2011;
posted ahead of print October 20, 2011. doi:10.1061/(ASCE)EM.1943-7889.0000347

recommended by Doherty (2000). The comparison suggested that the latter model overestimated wall instability displacement and wall lateral resistance for low values of mortar compressive strength. The observed differences between the predicted models using the aforementioned methods were partly due to the crack height being assumed differently.

ACKNOWLEDGEMENTS

The authors wish to acknowledge the financial support provided by the New Zealand Government via the Foundation for Research Science and Technology (FRST).

REFERENCES

ASCE (2007). *Seismic Rehabilitation of Existing Buildings, ASCE/SEI 41-06*. American Society of Civil Engineers, Reston, VA.

Blaikie, E. (1999). "Methodology for the assessment of face loaded unreinforced masonry walls under seismic loading." *Report No. C5643*, Opus International Consultants.

Brignola, A., Pampanin, S., and Podesta, S. (2009). "Evaluation and control of the in-plane stiffness of timber floors for the performance-based retrofit of URM buildings." *Bulletin of the NewZealand National Society for Earthquake Engineering*, 42(3), 204–221.

Clough, R. W., and Penzien, J. (2003). *Dynamics of structures (Third edition)*. pp. 145-148 Computers & Structures, Inc., Berkeley, CA, USA.

Journal of Engineering Mechanics. Submitted June 9, 2010; accepted October 17, 2011;
posted ahead of print October 20, 2011. doi:10.1061/(ASCE)EM.1943-7889.0000347

Derakhshan, H. (2011). "Seismic assessment of out-of-plane loaded unreinforced masonry walls," PhD thesis, Department of Civil and Environmental Engineering, The University of Auckland.

Derakhshan, H., Ingham, J. M., and Griffith, M. (2009). "Out-of-plane assessment of an unreinforced masonry wall: Comparison with the NZSEE recommendations." *New Zealand Society for Earthquake Engineering Technical Conference, 2009*, Christchurch, New Zealand. (in CD).

Doherty, K. T. (2000). "An investigation of the weak links in the seismic load path of unreinforced masonry buildings," PhD thesis, Faculty of Engineering of The University of Adelaide.

Griffith, M. C., Magenes, G., Melis, G., and Picchi, L. (2003). "Evaluation of out-of-plane stability of unreinforced masonry walls subjected to seismic excitation." *Journal of Earthquake Engineering*, 7(1), 141–169.

Ingham, J. M., Knox, C. L., Wilson, A. W., Elwood, K. J. "In-plane design loads for seismic assessment and retrofit of walls in unreinforced masonry buildings', *COMPDYN 2011, III ECCOMAS Thematic Conference on Computational Methods in Structural Dynamics and Earthquake Engineering*, M. Papadrakakis, M. Fragiadakis, V. Plevris (eds.), Corfu, Greece, 26–28 May.

Journal of Engineering Mechanics. Submitted June 9, 2010; accepted October 17, 2011;
posted ahead of print October 20, 2011. doi:10.1061/(ASCE)EM.1943-7889.0000347

Lawrence, S., Willis, C., Melkoumian, N., and Griffith, M. (2009). "Earthquake design of unreinforced masonry residential buildings up to 15 metres in height." *Australian Journal of Structural Engineering*, 10(1), 85–99.

Meisl, C. S., Elwood, K. J., and Ventura, C. E. (2007). "Shake table tests on the out-of-plane response of unreinforced masonry walls." *Canadian Journal of Civil Engineering*, 34(11), 1381–1392.

NZSEE (2006). *New Zealand Society for Earthquake Engineering (NZSEE): Assessment and Improvement of the Structural Performance of Buildings in Earthquakes*. Recommendations of a NZSEE Study Group on Earthquake Risk Buildings.

Priestley, M., Calvi, G., and Kowalsky, M. (2007). *Displacement-Based Seismic Design of Structures*. IUSS Press, Pavia, Italy.

Priestley, M. J. N. (1985). "Seismic behavior of unreinforced masonry walls." *Bulletin of the New Zealand National Society for Earthquake Engineering*, 18(2), 191–205.

Simsir, C. C. (2004). "Influence of diaphragm flexibility on the out-of-plane dynamic response of unreinforced masonry walls," PhD thesis, University of Illinois at Urbana-Champaign.

Journal of Engineering Mechanics. Submitted June 9, 2010; accepted October 17, 2011;
posted ahead of print October 20, 2011. doi:10.1061/(ASCE)EM.1943-7889.0000347

TABLES

TABLE 1: Illustrative examples of trilinear calculations

Ex.	t (mm)	h (mm)	f'_{fb} (MPa)	f'_j (MPa)	E (GPa)	ψ	Eq. 5 w_{cr} (kN/m)	Eq. 6 Δ_{ucr} (mm)	Eq. 28 PMR (%)	Eq. 29 F_i (kN)	Eq. 30 Δ_{ins} (mm)	Eq. 33 Δ_1 (mm)	Eq. 34 Δ_2 (mm)
W1	210	5000	0.2	1	2	0	0.6	3.1	77	1.8	202	8	62
W2	210	4000	0.2	8	4.5	0	0.9	0.8	82	1.9	209	8	54
W3	310	5000	0.2	1	2	1	1.8	2.9	70	10.2	212	8	79
W4	310	4000	0.2	8	4.5	0	1.9	0.6	82	4.0	309	12	80

Journal of Engineering Mechanics. Submitted June 9, 2010; accepted October 17, 2011;
posted ahead of print October 20, 2011. doi:10.1061/(ASCE)EM.1943-7889.0000347

NOTATIONS

a= Rectangular stress block length (mm);
B= Diaphragm width (mm);
β= Crack height ratio;
c_1= Rectangular stress block length coefficient;
$\Delta_m, \Delta_t, \Delta_{ucr}, \Delta, \Delta_1, \Delta_2, \Delta_{ins}$= Displacement parameters (mm);
E= Masonry modulus of elasticity (GPa);
$f_j^{'}$= Mortar compressive strength (MPa);
$f_{fb}^{'}$= Masonry bond strength (MPa);
$\hat{F}_0$= Predicted (bilinear) maximum wall resistance (kN);
F_{cr}= Cracking force (kN);
F_i= Idealized maximum wall resistance (kN);
$F_{\max}$= Maximum wall resistance (kN);
h= Wall clear height (mm);
H_A, H_C= Reaction forces;
I_{cr}= Cracked wall moment of inertia (mm^4);
I_g= Wall gross moment of inertia (mm^4);
K_D= Top support stiffness (kN/mm);
K_{ucr}, K_1= Uncracked and cracked wall initial stiffness (N/mm);
L = Diaphragm span equal to wall length (mm);
l_e= Effective wall length (mm);
m_0= wall mass per unit area;
M = Bending moment;
O, O_e= Overburden load (kN);
p = Depth of mortar pointing (mm)
PMR, PMR_{emp}= Percentage of maximum wall rigid resistance;
σ^T= Tensile stress of extreme fiber
t, t_n = Nominal and effective wall thicknesses (mm);
$w_{\text{cr}}, \hat{w}_{\max}, w_{\max}, w, w_e$ = Uniform out-of-plane force (kN/m);
W, W_e= Wall weight (kN);
ψ= Overburden ratio;

Journal of Engineering Mechanics. Submitted June 9, 2010; accepted October 17, 2011;
posted ahead of print October 20, 2011. doi:10.1061/(ASCE)EM.1943-7889.0000347

LIST OF TABLES

Journal of Engineering Mechanics. Submitted June 9, 2010; accepted October 17, 2011;
posted ahead of print October 20, 2011. doi:10.1061/(ASCE)EM.1943-7889.0000347

LIST OF FIGURES

Figure 1

Journal of Engineering Mechanics. Submitted June 9, 2010; accepted October 17, 2011;
posted ahead of print October 20, 2011. doi:10.1061/(ASCE)EM.1943-7889.0000347

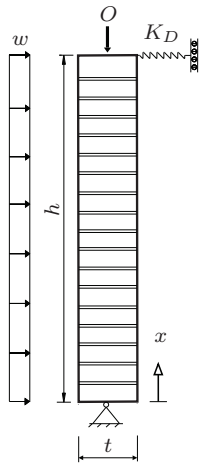

FIG. 1: Out-of-plane wall section

Figure 2

Journal of Engineering Mechanics. Submitted June 9, 2010; accepted October 17, 2011;
posted ahead of print October 20, 2011. doi:10.1061/(ASCE)EM.1943-7889.0000347

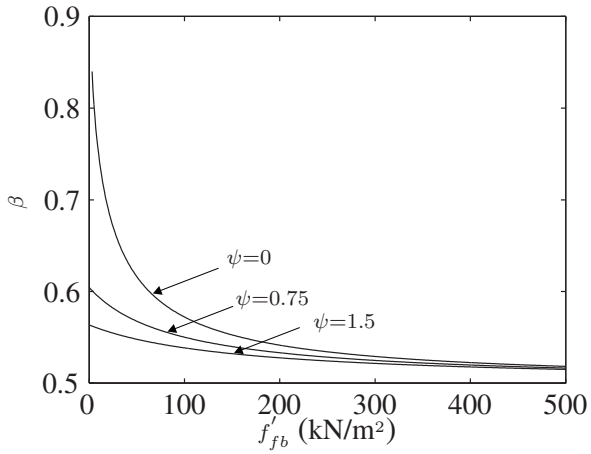

FIG. 2: Variation of β versus overburden and masonry bond strength

Figure 3

Journal of Engineering Mechanics. Submitted June 9, 2010; accepted October 17, 2011;
posted ahead of print October 20, 2011. doi:10.1061/(ASCE)EM.1943-7889.0000347

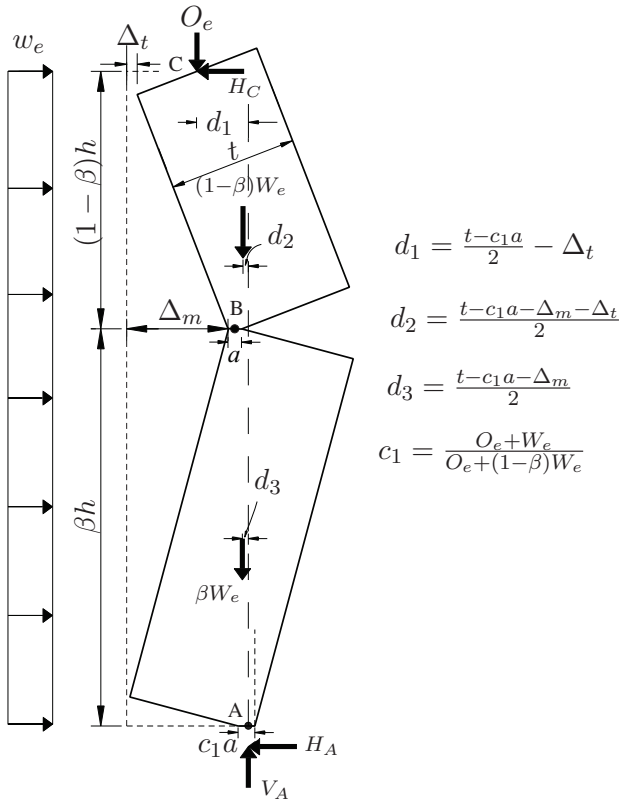

FIG. 3: Deformed shape of wall at mid-span

Figure 4

Journal of Engineering Mechanics. Submitted June 9, 2010; accepted October 17, 2011;
posted ahead of print October 20, 2011. doi:10.1061/(ASCE)EM.1943-7889.0000347

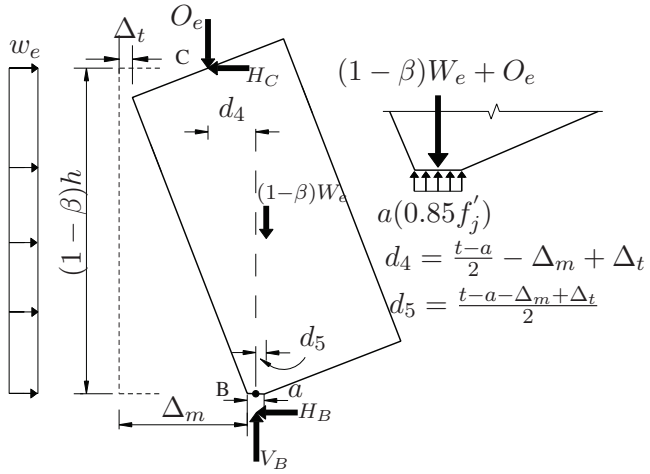

FIG. 4: Top free body

Figure 5

Journal of Engineering Mechanics. Submitted June 9, 2010; accepted October 17, 2011;
posted ahead of print October 20, 2011. doi:10.1061/(ASCE)EM.1943-7889.0000347

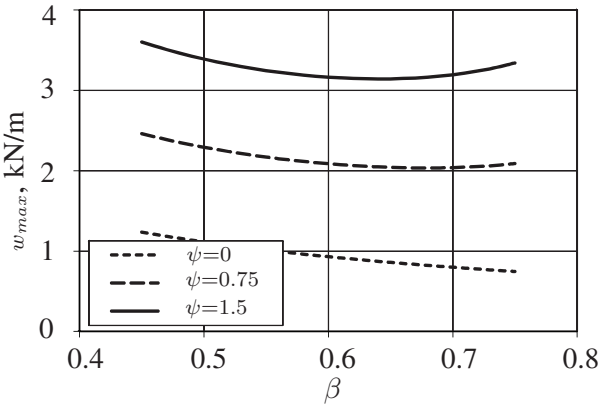

FIG. 5: Dependency of wall lateral resistance on β

Figure 6

Journal of Engineering Mechanics. Submitted June 9, 2010; accepted October 17, 2011;
posted ahead of print October 20, 2011. doi:10.1061/(ASCE)EM.1943-7889.0000347

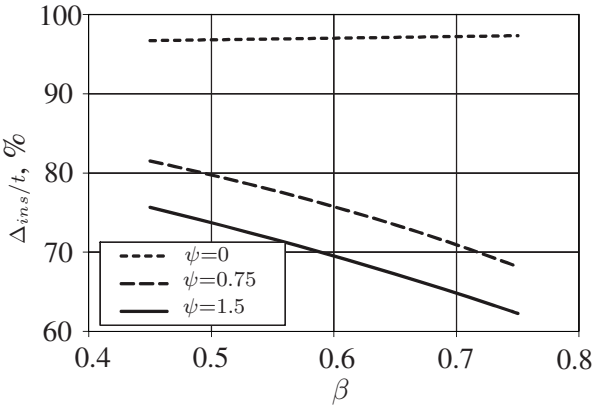

FIG. 6: Dependency of wall instability displacement on β

Figure 7

Journal of Engineering Mechanics. Submitted June 9, 2010; accepted October 17, 2011;
posted ahead of print October 20, 2011. doi:10.1061/(ASCE)EM.1943-7889.0000347

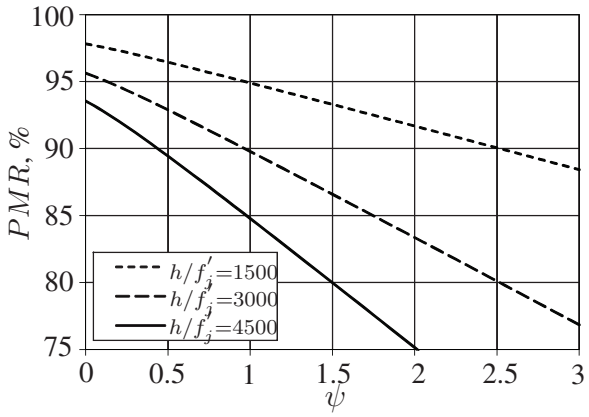

FIG. 7: Dependency of the percentage of maximum rigid resistance on overburden ratio

Figure 8

Journal of Engineering Mechanics. Submitted June 9, 2010; accepted October 17, 2011;
posted ahead of print October 20, 2011. doi:10.1061/(ASCE)EM.1943-7889.0000347

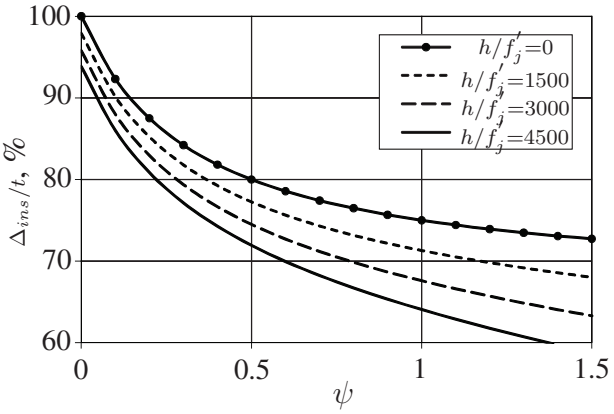

FIG. 8: Dependency of Δ_{ins} on overburden ratio

Figure 9

Journal of Engineering Mechanics. Submitted June 9, 2010; accepted October 17, 2011;
posted ahead of print October 20, 2011. doi:10.1061/(ASCE)EM.1943-7889.0000347

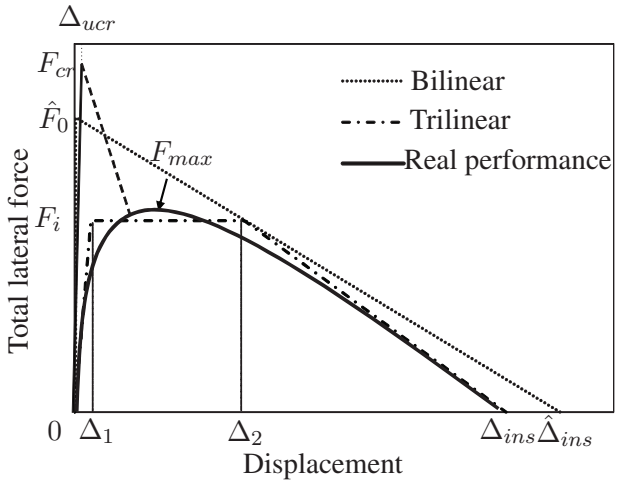

FIG. 9: Wall out-of-plane behaviour

Figure 10

Journal of Engineering Mechanics. Submitted June 9, 2010; accepted October 17, 2011;
posted ahead of print October 20, 2011. doi:10.1061/(ASCE)EM.1943-7889.0000347

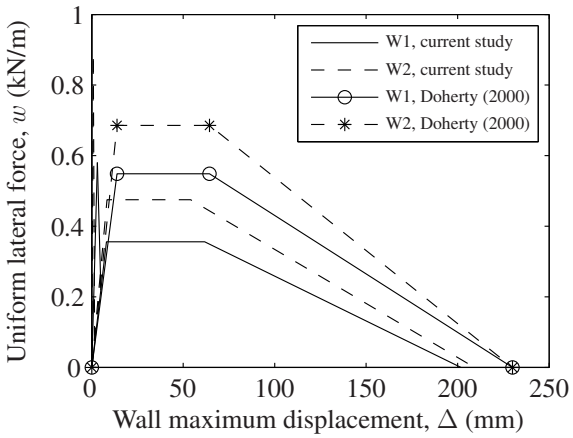

FIG. 10: Illustrative examples for two-leaf walls

Figure 11

Journal of Engineering Mechanics. Submitted June 9, 2010; accepted October 17, 2011;
posted ahead of print October 20, 2011. doi:10.1061/(ASCE)EM.1943-7889.0000347

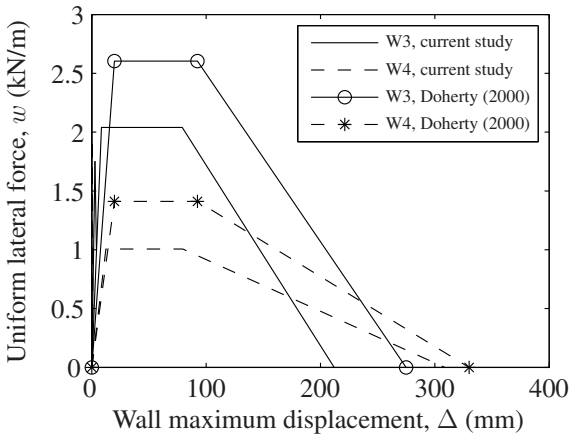

FIG. 11: Illustrative examples for three-leaf walls

Journal of Engineering Mechanics. Submitted June 9, 2010; accepted October 17, 2011;
posted ahead of print October 20, 2011. doi:10.1061/(ASCE)EM.1943-7889.0000347

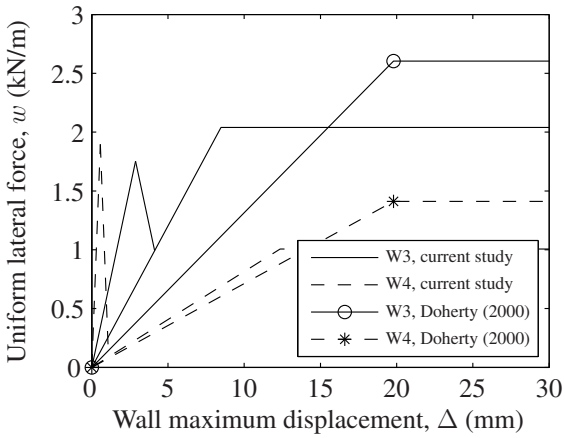

FIG. 12: Comparison between cracking force and maximum rocking force